De Novo Design of a Copper(II)-Binding Helix−Turn−Helix Chimera: The Prion Octarepeat Motif in a New Context†

S. Brookhart Shields and Sonya J. Franklin*

Department of Chemistry, University of Iowa, Iowa City, Iowa 52242

Received July 8, 2004; Revised Manuscript Received October 8, 2004

ABSTRACT: A chimeric Cu-binding peptide has been designed on the basis of a turn substitution of the prion (PrP) octarepeat Cu-binding site into the engrailed homeodomain helix−turn−helix motif (HTH). This system is a model for the investigation of a single PrP Cu-binding site in a defined protein context. The 28-mer Cu-HTH peptide P7 spectroscopically mimics the PrP octarepeat (P7 = TERRRQQLSHGGGWGEAQIKIWFQNKRA). The Cu(II)-binding affinity of P7 was determined by ESI-MS and tryptophan fluorescence titrations to be $K_d = 2.5 \pm 0.7$ μM at pH = 7.0. The quenching of fluorescence of the Trp within the binding loop (underlined above) is pH dependent and highly specific for Cu(II). No Trp quenching was observed in the presence of divalent Zn, Mn, Co, Ni, or Ca ions, and ESI-MS titrations confirmed that these divalent ions do not appreciably bind to P7. The EPR spectrum of Cu(II)-P7 shows that the Cu environment is axial and consistent with 6-coordinate $N_3O(H_2O)_2$ or $N_4(H_2O)_2$ coordination ($A_{||} = 172 \times 10^{-4}$ cm^{-1}; $g_{||} = 2.27$), very similar to that of the PrP octarepeat itself. Also like PrP, circular dichroism studies show that apo P7 is predominantly disordered in solution, and the structure is slightly enhanced by Cu binding. These data show the Cu-PrP HTH peptide reproduces the Cu-binding behavior of a single PrP octarepeat in a new context.

De novo protein design is an approach that is coming into its own as a tool for the bioinorganic chemist, as a way to both isolate and investigate metal sites in defined protein contexts and build or combine activity and selectivity in unique ways. Within the context of designing an artificial nuclease, we have utilized de novo design to investigate fundamental questions about metalloprotein structure and function. In particular, the inherent stability of supersecondary structures in proteins and the contextual reactivity of a given metal-binding amino acid sequence are of interest. We have previously demonstrated that an EF-hand Ca-binding loop can be incorporated into a helix−turn-helix motif (HTH) with retention of the structure, DNA-binding affinity, and metal-binding properties (*1*−*3*). Lanthanide metallopeptides designed on the basis of structurally similar turns fold as predicted and catalyze the cleavage of phosphate esters and DNA (*4*), with modest sequence preference (*5*). These data show that an active metal site can be designed into a new context, incorporating both reactivity and targeting functions and retaining folded structure.

Our work with EF-hand binding sites showed that, with a well-organized turn, the HTH is a robust scaffold upon which to design a new fold comprising fragments of very similar α−α corner structures (∼orthogonal helices flanking a turn) (*6*). We therefore postulated that the turn could potentially be modularly substituted by other metal-binding sites besides Ca(II) sites and have thus incorporated a portion (underlined) of the unusual prion octarepeat Cu(II)-binding sequence (PHGGGWGQ) into the HTH motif of the engrailed homeodomain. If this relatively small, HTH system can structurally accommodate the Cu turn and maintain the Cu-binding properties, this opens the possibility of designing larger, better folded, soluble prion model proteins to test the reactivity of Cu sites systematically. De novo designed copper-binding proteins have been effectively utilized to investigate the structure and function of a variety of metalloprotein Cu sites (recently reviewed in refs *7*−*9*), and thus we chose to apply this method to the prion site.

The prion protein (PrP), a highly conserved glycoprotein responsible for a range of transmissible spongiform encephalopathy diseases (TSE), has been shown to be a Cu-binding protein (*10*−*13*). The octarepeat sequence occurs sequentially four times in the N-terminus of the human PrP and is predominantly disordered in the absence of copper (*11*, *14*, *15*). Each octarepeat can accommodate one Cu(II), with low micromolar affinity (*16*, *17*), but under some conditions metal-based dimerization of this N-terminal region may catalyze the pathogenic misfolding of the C-terminal domain of the prion protein (*16*). Despite the interest and attention given this important protein, its natural function and the explicit mechanisms triggering neurodegenerative disease remain unknown. It is postulated that Cu-redox chemistry is involved in the function of PrP, in either the normal or pathogenic forms, but no consensus has emerged for the role of the metal. Defining the role of copper binding is a critical keystone in understanding prion physiology and pathogenicity, yet the unstructured, repetitive, multicomponent nature of the Cu-binding N-terminus presents limitations in investigating the inherent function of the metal site. This model system will allow us to test the speculated reactivity [such

† This work was supported by the University of Iowa Carver Research Foundation.

* To whom correspondence should be addressed. E-mail: sonya-franklin@uiowa.edu. Phone: (319) 353-2244. Fax: (319) 335-1270.

10.1021/bi048555k CCC: $27.50
Published on Web 12/04/2004

as Cu(II) reduction and superoxide dismutase activity] and the spectroscopy of the isolated site within a controlled scaffold. Additionally, this site may represent a new approach to nuclease design, utilizing an essential metal for DNA-cleavage applications. We find that a peptide that comprises the HTH motif of the engrailed homeodomain and the prion Cu(II) site binds copper and involves the adjacent Trp residue in or near the binding site as does the prion protein (*10*).

MATERIALS AND METHODS

Peptides and Reagents. Peptide P7 was synthesized by standard Fmoc solid-phase chemistry and HPLC purified to >95% purity (Caltech Peptide Facility). Reagent grade metal salts ($CuCl_2$, $CuSO_4$, $CaCl_2$, $CoCl_2$, $MgCl_2$, $MnCl_2$, $NiCl_2$, $ZnCl_2$) and buffers were supplied by Sigma-Aldrich, and all other solvents and reagents were from Fisher Scientific and used as received. All solutions were made with deionized distilled water (MilliQ 18 mΩ). Stock metal solutions were prepared fresh by weight prior to use.

EPR Spectroscopy. Electron paramagnetic resonance spectra were collected on a Brüker X-band 300-EMX spectrometer at 77 K under the following conditions: 9.29 GHz microwave frequency, 1.6 kHz modulation frequency, 20 mW microwave power, 5.0 G modulation amplitude, 2987.8 G center field, 1200 G sweep width, and 163.84 ms time constant. Solutions contained 200 μM peptide, 200 μM $CuSO_4$, 25 mM 3-(*N*-morpholino)-2-hydroxypropanesulfonic acid (MOPS) buffer at pH 6.8, 25 mM NaCl, 40% glycerol, and 10% MeOH. Simfoni 1.0 software (Brüker) was used to simulate the data and calculate the *g* and *A* values.

Fluorescence Spectroscopy. Tryptophan emission spectroscopy was followed as a function of divalent metal. Peptide solutions were excited at 295 nm, and the emission due to Trp was monitored at 350 nm with an Aminco-Bowman Series 2 fluorimeter. Quenching experiments were performed using solutions containing 5 μM peptide, 50 mM buffer, and 50 mM NaCl over a range of pH conditions modulated by the following buffers: sodium acetate buffer (pH = 4, 5), 2-(*N*-morpholino)ethanesulfonic acid buffer (MES) (pH = 6), 3-(*N*-morpholino)-2-hydroxypropanesulfonic acid buffer (MOPS) (pH = 7), and *N*-ethylmorpholine buffer (NEM) (pH = 8). The initial fluorescence intensities of the solutions were measured, 10 equiv of the specified divalent metal chloride salts was added (Cu, Ca, Co, Mg, Mn, Ni, Zn), and the solutions were incubated for 15 min before the final emission was measured. The difference in the final and initial intensity was normalized and corrected for a slight loss in intensity of the apopeptide (<10%) over time. The data in Figure 5 represent averages of five samples. Copper titrations were performed over a range of peptide concentrations (1−20 μM P7, with 0.1−10 equiv of $CuCl_2$) at pH 7.5 in either MOPS or NEM buffers, with and without NaCl (the addition of 50 mM salt did not affect the apparent K_d). The loss in fluorescence intensity with the addition of copper was fitted to a 1:1 associate model (*4*) using a nonlinear least-squares fit algorithm (SigmaPlot), including a linear correction for collisional quenching at high [Cu] (*18*).

Circular Dichroism Spectroscopy. Circular dichroism spectra were collected on an Olis Cary-17 DS conversion spectrophotometer. Spectra were recorded under a nitrogen purge in a 1 mm cuvette at 0.5 nm per point and an integration time of 0.2 s/point. Solutions contained 50 μM peptide, 10 mM *N*-ethylmorpholine buffer (pH 7.5), and 10 mM NaCl, with and without 1 equiv of $CuCl_2$. Additionally, spectra were collected in 25% trifluoroethanol (TFE) under the same buffer conditions.

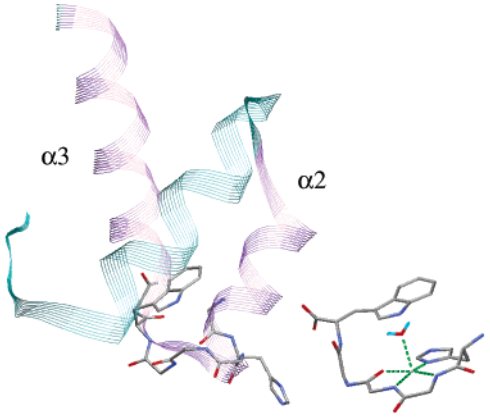

P7 ***TERRRQQLSHGGGWGEAQIKIWFQNKRA***

FIGURE 1: Crystal structure of pentapeptide Cu(II)-HGGGW (ref *16*; right) and a model based on the crystal structure of the engrailed homeodomain (1ENH; left) showing the proposed binding modes for the P7 chimera. The sequence of P7 (with the loop substitution underlined) is given below. The side chains of residues 36−41 of the published engrailed structure have been altered in the computer model to reflect the P7 sequence, but no minimization from the parental crystal structure was done. The purple helices represent the sequences of engrailed included in the peptide (α2, α3).

Electrospray Ionization Mass Spectrometry. Electrospray ionization mass spectrometry data (ESI-MS) were collected on a Thermo Finnigan LCQ Deca spectrometer (University of Iowa High-Resolution Mass Spectrometry Core Facility; NIH Grant 510 RR13799-01). Solutions contained 2−5 μM P7 peptide, 5 mM NEM buffer at pH 7.0, and 15% MeOH with 0−10 equiv of $CuCl_2$. Solutions were incubated at room temperature for 1 h and infused into the spectrometer system for 20 min at 5 μL/min prior to data collection. The following conditions were optimized to maximize the signal-to-noise ratio: spray voltage, 4.2 kV; sheath gas, 30 units; capillary temperature, 225 °C; capillary voltage, 34 V. The sum of the intensities of the predominant charge states' envelopes of the bound and unbound peptide was used to calculate the concentration of free copper (+2 and +3 charge states were generally the only ions of significant intensity). These quantities were then used to calculate K_d directly, where $K_d = ([Cu_{free}][peptide_{free}])/[Cu\text{-}peptide]$ (*19*). Other divalent ions were screened for binding under similar conditions [1.5 μM P7, 15 μM M(II)].

RESULTS AND DISCUSSION

Unlike our earlier EF-hand/HTH chimeric designs, the apparent Cu-binding site of the prion protein is the same length as the native turn in the DNA-binding motif, and thus no expansion of the turn is necessary upon loop substitution. A model based on the crystal structure of Cu(II)-HGGGW (Figure 1) (*16*) suggests that the Cu could bind to the modified turn of the engrailed homeodomain in a similar mode, with little perturbation of the HTH supersecondary structure. Therefore, a peptide comprising helices 2 and 3 of the engrailed homeodomain (residues T_{27}−S_{35} and E_{42}−

Table 1: EPR Parameters for Various Cu(II) PrP Peptides

peptide	$g_{\|\|}$	$g_{\perp}$	$A_{\|\|} \times 10^{-4}$ (cm^{-1})	$g_{\|\|}/A_{\|\|}$ (cm)	pH
P7 chimera[a]	2.27	2.03	172	132	6.8
PrP(58−91)[b]	2.26	2.05	195	116	6.6−7.7
PrP(57−91)[c]	2.27	2.06	179	127	6.75
PrP(57−91)[c]	2.23	2.06	163	137	7.45

[a] This work. [b] Wright (*17*). [c] Millhauser (*12*).

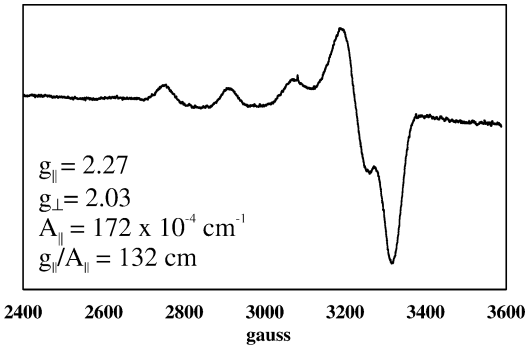

FIGURE 2: X-band EPR of CuP7 (200 μM) in 25 mM MOPS buffer, pH 6.8, 25 mM NaCl, 40% glycerol, and 10% MeOH. Spectra were collected at 77 K, $\nu_0 = 9.29$ GHz, with a sweep width of 1200 G.

A_{54}, respectively) and the central six amino acids of the prion octarepeat was prepared.

Copper-Binding Site and Affinity. Copper(II) binding was demonstrated by Trp fluorescence titrations, EPR spectroscopy, and ESI mass spectrometry. The peptide was found to bind 1 equiv of Cu and to give an X-band EPR spectrum of CuP7 typical of the axial type 2 Cu(II) site within prions (Table 1) (*12*, *14*, *16*, *17*). According to Peisach−Blumberg correlations (*20*), the $A_{||}$ and $g_{||}$ values (Figure 2) are most consistent with N_3O or N_4 coordination, with weak axial ligands (solvent). The intermediate $A_{||}$ value and fairly small $g_{||}/A_{||}$ ratio suggest that the site tends toward 6-coordinate geometry, similar to the structure deduced for the prion octarepeat region (residues 57−91 of the prion protein).

The binding affinity of P7 for Cu(II) was estimated by fluorescence titration, following the emission intensity of the tryptophan residues as a function of added metal (Figure 3) (*4*, *18*). The intensity decreases significantly upon titration presumably due to structural changes upon binding that bring W_{15} into close proximity to the metal center, with subsequent fluorescence energy transfer to copper. The data were iteratively fit to give a conditional dissociation constant of $K_d^* = 200$ nM−2.0 μM for Cu(II) at pH 7.5 (error based on five repeated measurements) (*21*). Direct affinity constant determination from Stern−Volmer linear regression analysis was not possible under these conditions since $[Cu_{free}] \neq [Cu_{total}]$ and two Trp fluorophores are present in the peptide. However, a model with this approximation and incorporating pK_a estimates for amide NH and His imidazole gave qualitatively similar results (6 μM). Stern−Volmer analysis suggested significant contribution (up to 35%) from Cu-Trp collisional quenching at high [Cu] (*18*).

The conditional binding affinity of P7 for Cu(II) is similar to that of the prion octarepeat region (residues 58−91) under similar buffer and pH conditions (*10*, *17*, *19*) and, like the prion system, is quite sensitive to buffer and pH (Supporting Information, Table S1). The prion protein has been reported to bind Cu(II) with affinities typically ranging from 0.5 to 14 μM, although there is one report of 10^{-14} affinity (*22*). The formation of the ML species is dependent on the protonation conditions of the ligand, which at pH 7.4 is estimated to exist as a mixture of approximately 90% H_2L and 10% H_3L (considering donor group deprotonations only), with only a very small fraction of fully deprotonated ligand ($\alpha_L \approx 10^{-13}-10^{-14}$). This fractionation constant is based on a conservative estimate of the NH amide pK_a of 13−15 and on the measured pK_a of the His imidazole, found to be 6.1 by ^{1}H NMR pH titration of the free peptide (Supporting Information, Figure S1).

Since the observed conditional binding constant is a sum of affinities for Cu(II) and protons, the proton-dependent formation constant (K_f^*) includes the contributions of pH to the fraction of available free ligand ($K_f^* = \alpha_L K_f$). Thus, an estimate of the thermodynamic formation constant of CuP7 is $K_f = 10^{19}-10^{20}$ M^{-1}. In practice, this affinity can only be measured as a competition with another ligand of known affinity, which may contribute to the apparent inconsistencies in the literature. The reported femtomolar affinities of the Cu-albumin Gly-Gly-His site (*23*) and for the prion octarepeat in the presence of glycine (*22*) were calculated from competitive measurements. Though the thermodynamic Cu-binding affinity of the octarepeat and P7 is also predicted to be very strong, micromolar dissociation constants result at physiological pH.

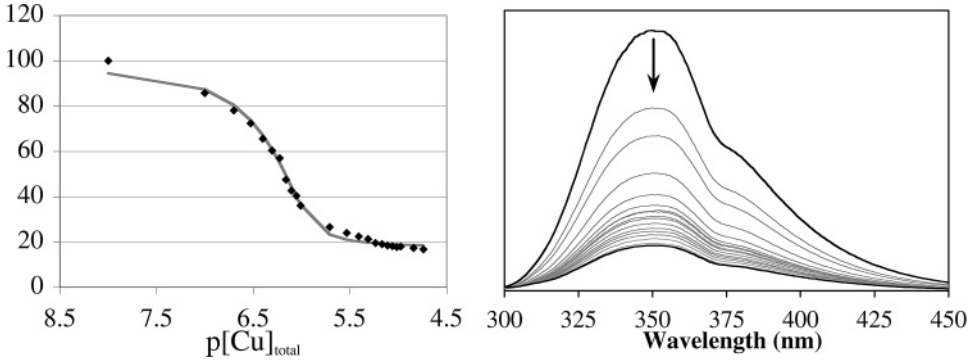

FIGURE 3: Left: Fluorescence intensity at 350 nm (points; $\lambda_{ex} = 295$ nm) and fit (line) for the titration of P7 with Cu(II). Titrations were performed at [P7] between 1 and 20 μM peptide (shown at 20 μM). Right: Tryptophan emission spectra of peptide P7 as a function of added $CuCl_2$, pH = 7.5, 50 mM MOPS. Data were iteratively fit to a 1:1 association model as described previously (*4*). Cu(II) $K_d = 200$ nM−2.0 μM with five repeated trials. A Stern−Volmer linear regression analysis at high copper concentrations yielded a K_{SV} of 4200 M^{-1} and suggested that the fraction of fluorescence change due to binding and structural changes was approximately 65% (see ref *18*). Affinities are somewhat weaker in *N*-ethylmorpholine buffer (2−3 μM).

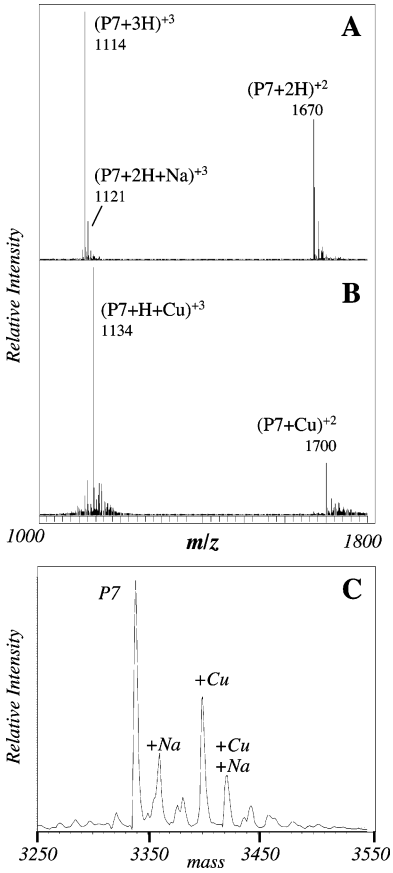

FIGURE 4: ESI mass spectra of CuP7. (A) Mass spectrum of 10.0 μM apo-P7 (2+ and 3+ charge states shown). (B) Mass spectrum of CuP7 [10.0 μM P7:12.0 μM Cu(II); 2+ and 3+ charge states shown]. (C) Deconvolution spectrum of all species at substoichiometric Cu(II) concentrations, showing P7 and the sodium and copper adducts [10.0 μM P7:6.0 μM Cu(II)]. Summations of each charge species and its sodium adducts over a range of Cu concentrations were used to calculate a binding constant of $K_d = 2.5 \pm 0.7$ μM. The stoichiometry of Cu:P7 was found to be 1:1 even up to 20-fold excess Cu(II) concentrations.

The binding affinity of P7 for Cu was determined by ESI-MS to corroborate the estimates calculated from Trp fluorescence titrations (Figure 4). Solutions of peptide with increasing amounts of $CuCl_2$ were prepared in 15% MeOH (5 mM *N*-ethylmorpholine, pH 7.0) and preincubated at room temperature for 1 h prior to data collection. Spray voltage, capillary voltage and temperature, and flow rate were adjusted to maximize the signal-to-noise ratio (2+ and 3+ ions were generally most intense). These data showed that only 1 equiv of Cu associated with the peptide even up to 20-fold excess metal. The total concentration of copper ($[Cu_{tot}] = [CuP7] + [Cu_{free}]$) and the sums of the intensities of the bound ([CuP7]) and unbound ($[P7_{free}]$) states were used to calculate K_d at each point ($K_d = ([P7_{free}][Cu_{free}]/[CuP7] = 2.5 \pm 0.7$ μM). The difference in ionization response of the two species is apparently small, since the calculated affinity was found to be invariant over a wide concentration range (*24*).

Trp Fluorescence Quenching and Selectivity for Cu(II). One hallmark of the unusual Cu-prion site is the involvement of a key Trp residue in the second shell. This Trp is critical to Cu binding in the native site, and its presence serves to favor the binding of more nitrogen donors and therefore fewer oxygen ligands [it should be noted that this conclusion is based on truncation rather than substitution studies of octarepeat peptides (*12*)]. Notably, strong Trp fluorescence quenching is a characteristic of the PrP octarepeat site (*10*). As shown in Figure 5, a dramatic change in tryptophan emission intensity occurred upon Cu(II) addition to P7 ($\approx$80% decrease at pH 8). This is consistent with significant changes in the Trp electronic environment facilitating fluorescence energy transfer, such as would be expected for W_{14} hydrogen bonding to a coordinated water molecule as observed in the pentapeptide structure (Figure 1) (*25*−*27*). As was observed for the PrP itself (*10*), this effect in the designed HTH chimera is unique to Cu(II) and is pH dependent, which supports the postulate that binding occurs upon deprotonating the His_{10} imidazole and backbone amide nitrogens. A range of other divalent metal ions were tested (Figure 5), but like PrP, only Cu(II) shows any appreciable Trp quenching (*28*). This suggests the prion site in this new context may also be preorganized to direct W_{14} toward Cu(II), perhaps interacting with an axial water ligand. On the basis of the Trp fluorescence data alone, the possibility remained that Ni(II), Co(II), or even Zn(II) may bind to the site but not significantly perturb the adjacent Trp residue or cause peptide folding. Binding studies of the various divalent metals by ESI mass spectrometry were undertaken to address this question. In all cases tested except Cu(II), no appreciable metal-bound peak was observed in the ESI-MS up to 10 equiv of divalent metal. From these data, conservative lower limits for the dissociation constants were calculated to be $K_d \geq 280$ μM for Zn(II) (7.0 $\pm$ 2.0% metalated peptide) and $K_d \geq 340$ μM for Ni(II) (5.9 $\pm$ 0.2% metalated peptide) under the conditions tested (*29*). Accurate estimates could not be made for the remaining divalent metal ions, as no metal-bound peak could be reproducibly observed.

Structure of the Motif. Circular dichroism spectroscopy (Figure 6) shows that, like the PrP N-terminus, the apopeptide P7 is predominantly unfolded in solution, and the binding of Cu(II) minimally increases overall secondary structure. A similar effect is seen by ^{1}H NMR, with modest spectral changes suggesting that copper coordination is not accompanied with the induction of significant long-range helicity. However, the broadening of the His_{10} aromatic peaks upon Cu(II) addition further indicates that this residue is involved in binding (data not shown). The lack of secondary structure is not unexpected, as the Gly-rich prion turn is predicted to be much more flexible than the evolutionarily optimized turn it replaces in engrailed. Additionally, in the prion site itself, a proline residue is required to nucleate the turn (*14*, *30*). Although Cu binding likely organizes the central residues of the designed peptide, this does not result in significant α-helical propagation at the termini, since the structure is already somewhat destabilized by isolating the motif from the full domain. However, if local secondary structure is stabilized with trifluoroethanol (TFE), a solvent that promotes helical structure, copper binding significantly increases the overall α-helicity observed relative to apo P7 and results in a qualitatively helical (HTH-like) CD spectrum. The structural equilibrium of the peptide is apparently near the balance between folded and unfolded, because CuP7 can accommodate a folded structure when perturbed by only mild TFE conditions. It is notable that some increase in the intensity of a negative band at 220 nm was reported in the CD spectrum of the simple pentapeptide HGGGW upon

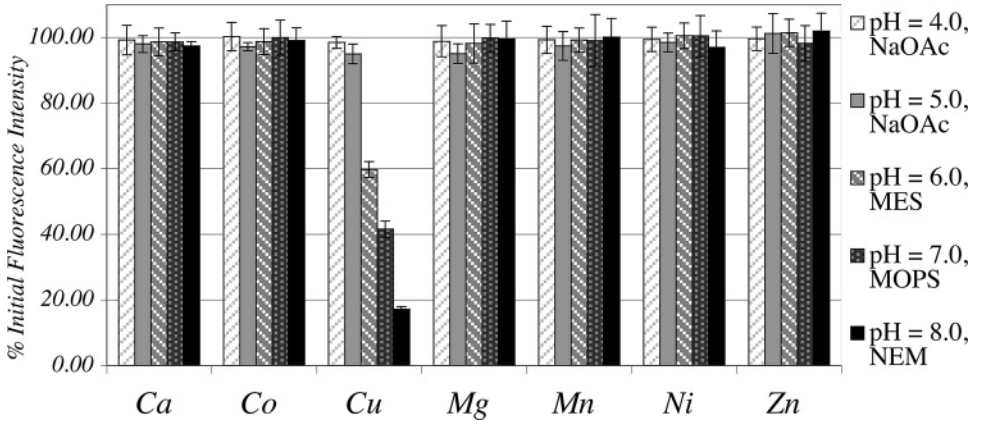

FIGURE 5: Fluorescence intensity of the Trp emission at 350 nm (290 nm excitation) as a function of pH (50 mM buffer, 50 mM NaCl) for various divalent metal chlorides. Data are corrected for changes (≤10%) in apopeptide emission over the course of the experiment, and error bars represent five repetitions. The emission is quenched by Cu(II) binding but not by other metal ions.

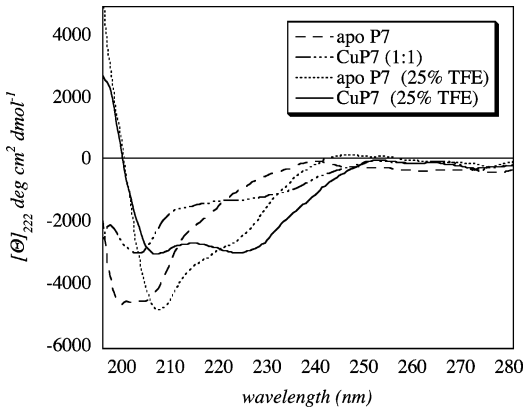

FIGURE 6: Circular dichroism spectra of peptide P7 (50 μM) with and without added $CuCl_2$ in the presence and absence of 25% TFE. Conditions: 10 mM *N*-ethylmorpholine, 10 mM NaCl, pH 7.5.

copper binding (*31*), and thus in the absence of TFE, changes in local structure of the binding site upon Cu coordination could also contribute to the observed CD signal changes. Taken together, these data suggest that CuP7 can sample a HTH structure similar to a fragment of the parental engrailed domain (modeled in Figure 1), and Cu binding organizes the core region around the turn and favors this fold. Although CuP7 is likely on average not extensively helical in solution, the HTH motif appears amenable to this "turn-substitution" modeling approach for the prion copper-binding site. Further studies are underway to optimize the chimeric design by incorporating the turn within the context of the larger homeodomain to enhance overall structure and the utility of the model.

CONCLUSIONS

A designed prion-model peptide has been prepared on the basis of a metallo-turn substitution into the helix−turn−helix motif. The strong, axial complexation of Cu(II) appears to involve His and Trp residues, the latter potentially involved in second shell hydrogen-bonding interactions. The overall structure of the peptide is enhanced by nonaqueous solvent and copper binding, showing that the HTH motif can accommodate metal-binding sites other than Ca−EF-hand sites. These data suggest that the designed peptide P7 binds Cu(II) with local geometry similar to the Cu(II)-HGGGW crystal structure and the inferred structure of the octarepeat prion site itself. The prion Cu-binding site is apparently contextually insensitive to flanking sequence, with little change in local structure, binding affinity, or pH dependence relative to the isolated octarepeat motif. Thus, the designed HTH/PrP chimeric system may be a useful model to understand the structural flexibility and reactivity of a single prion site, isolated in a new context.

ACKNOWLEDGMENT

We thank Prof. Garry R. Buettner for assistance with EPR spectroscopy, Dr. Lynn Teesch for mass spectrometry advice, and Profs. Johna Leddy and Lei Geng for many useful discussions.

SUPPORTING INFORMATION AVAILABLE

One table listing the first Cu(II) dissociation constant for various PrP peptides and one figure showing ^{1}H NMR of the His_{10} imidazole of peptide P7. This material is available free of charge via the Internet at http://pubs.acs.org.

REFERENCES

1. Welch, J. T., Kearney, W. R., and Franklin, S. J. (2003) Lanthanide-Binding HTH Peptides: Solution Structure of a Designed Metallonuclease, *Proc. Natl. Acad. Sci. U.S.A. 100*, 3725−3730.
2. Kim, Y., Welch, J. T., Lindstrom, K. M., and Franklin, S. J. (2001) Chimeric HTH Motifs Based on EF-Hands, *J. Biol. Inorg. Chem. 6*, 173−181.
3. Jain, S., Welch, J. T., Horrocks, W. D., Jr., and Franklin, S. J. (2003) Europium Luminescence of EF-hand HTH Chimeras: Impact of pH and DNA-Binding on Europium Coordination, *Inorg. Chem. 42*, 8098−8104.
4. Sirish, M., and Franklin, S. J. (2002) Hydrolytically Active Eu(III) and Ce(IV) EF-Hand Peptides, *J. Inorg. Biochem. 91*, 253−258.
5. Kovacic, R. T., Welch, J. T., and Franklin, S. J. (2003) Sequence Preference in DNA Cleavage by a Chimeric Metallopeptide, *J. Am. Chem. Soc. 125*, 6656−6662.
6. Efimov, A. V. (1996) A structural tree for α-helical proteins containing α−α-corners and its application to protein classification, *FEBS Lett. 391*, 167−170.
7. Barker, P. D. (2003) Designing redox metalloproteins from bottom-up and top-down perspectives, *Curr. Opin. Struct. Biol. 13*, 490−499.
8. Kennedy, M. L., and Gibney, B. R. (2001) Metalloprotein and redox protein design, *Curr. Opin. Struct. Biol. 11*, 485−490.
9. Lu, Y., Berry, S. M., and Pfister, T. D. (2001) Engineering Novel Metalloproteins: Design of Metal-Binding Sites into Native Protein Scaffolds, *Chem. Rev. 101*, 3047−3080.

10. Stöckel, J., Safar, J., Wallace, A. C., Cohen, F. E., and Prusiner, S. B. (1998) Prion Protein Selectively Binds Copper(II) Ions, *Biochemistry 37*, 7185−7193.
11. Prusiner, S. B. (1998) Prions, *Proc. Natl. Acad. Sci. U.S.A. 95*, 13363−13383.
12. Aronoff-Spencer, E., Burns, C. S., Avdievich, N. I., Gerfen, G. J., Peisach, J., Antholine, W. E., Ball, H. L., Cohen, F. E., Prusiner, S. B., and Millhauser, G. L. (2000) Identification of the Cu^{2+} Binding Sites in the N-Terminal Domain of the Prion Protein by EPR and CD Spectroscopy, *Biochemistry 39*, 13760−13771.
13. Millhauser, G. L. (2004) Copper Binding in the Prion Protein, *Acc. Chem. Res. 37*, 79−85.
14. Burns, C. S., Aronoff-Spencer, E., Legname, G., Prusiner, S. B., Antholine, W. E., Gerfen, G. J., Peisach, J., and Millhauser, G. L. (2003) Copper Coordination in the Full-Length, Recombinant Prion Protein, *Biochemistry 42*, 6794−6803.
15. Lehmann, S. (2002) Metal ions and prion diseases, *Curr. Opin. Chem. Biol. 6*, 187−192.
16. Burns, C. S., Aronoff-Spencer, E., Dunham, C. M., Lario, P., Avdievich, N. I., Antholine, W. E., Olmstead, M. M., Vrielink, A., Gerfen, G. J., Peisach, J., Scott, W. G., and Millhauser, G. L. (2002) Molecular Features of the Copper Binding Sites in the Octarepeat Domain of the Prion Protein, *Biochemistry 41*, 3991−4001.
17. Viles, J. H., Cohen, F. E., Prusiner, S. B., Goodin, D. B., Wright, P. E., and Dyson, H. J. (1999) Copper binding to the prion protein: Structural implications of four identical cooperative binding sites, *Proc. Natl. Acad. Sci. U.S.A. 96*, 2042−2047.
18. Kramer, M. L., Kratzin, H. D., Schmidt, B., Römer, A., Windl, O., Liemann, S., Hornemann, S., and Kretzschmar, H. (2001) Prion Protein Binds Copper within the Physiological Concentration Range, *J. Biol. Chem. 276*, 16711−16719.
19. Whittal, R. M., Ball, H. L., Cohen, F. E., Burlingame, A. L., Prusiner, S. B., and Baldwin, M. A. (2000) Copper binding to octarepeat peptides of the prion protein monitored by mass spectrometry, *Protein Sci. 9*, 332−343.
20. Peisach, J., and Blumberg, W. E. (1974) Structural Implications Derived from the Analysis of Electron Paramagnetic Resonance Spectra of Natural and Artificial Copper Proteins, *Arch. Biochem. Biophys. 165*, 691−708.
21. Loss of Trp intensity was observed for apopeptide as well (≈10% over the course of a titration). Corrections for this effect did not appreciably change K_d but contribute to the higher reported errors in the nonlinear least-squares fit.
22. Jackson, G. S., Murray, I., Hosszu, L. L. P., Gibbs, N., Waltho, J. P., and Clarke, A. R. (2001) Location and properties of metal-binding sites on the human prion protein, *Proc. Natl. Acad. Sci. U.S.A. 98*, 8531−8535.
23. Lau, S. J., Kruck, T. P. A., and Sarkar, B. (1974) A Peptide Molecule Mimicking the Copper(II) Transport Site of Human Serum Albumin. A Comparative Study Between the Synthetic Site and Albumin, *J. Biol. Chem. 249*, 5878−5884.
24. Gabelica, V., Galic, N., Rosu, F., Houssier, C., and De Pauw, E. (2003) Influence of response factors on determining equilibrium association constants of noncovalent complexes by electrospray ionization mass spectrometry, *J. Mass Spectrom. 38*, 491−501.
25. The mechanism for fluorescence quenching in PrP has not been addressed. However, significant tryptophan fluorescence quenching via energy or electron transfer to copper has been reported for several other Cu-binding proteins with Trp residues proximal to the copper binding sites [azurin (*26*), N_2O reductase (*27*)].
26. Dooley, D. M., McGuirl, M. A., Rosenzweig, A. C., Landin, J. A., Scott, R. A., Zumft, W. G., Devlin, F., and Stephens, P. J. (1991) Spectroscopic Studies of the Copper sites in Wild-Type *Pseudomonas stutzeri* N_2O Reductase and in an Inactive Protein Isolated from a Mutant Deficient in Copper-Site Biosynthesis, *Inorg. Chem. 30*, 3006−3011.
27. Kroes, S. J., Canters, G. W., Gilardi, G., van Hoek, A., and Visser, A. J. W. G. (1998) Time-Resolved Fluorescence Study of Azurin Variants: Confromational Heterogeneity and Tryptophan Mobility, *Biophys. J. 75*, 2441−2450.
28. There are two tryptophan fluorophores in P7 (W_{14}, W_{22}), both of which may contribute to the emission spectrum. The changes in emission of W_{22} upon metal binding and peptide folding may be expected to be small (<15%), based on similar studies with designed Ln-binding chimeras, but probably contribute to the observed intensity decrease for P7. See ref *2*.
29. Conditions tested were 1.5 μM P7 and 15 μM Zn or Ni. Errors are based on five repeated measurements and are larger for Zn-(II) than Ni(II) because of the greater number of isotopes that must be summed.
30. Zahn, R. (2003) The Octapeptide Repeats in Mammalian Prion Protein Constitute a pH-dependent Folding and Aggregation Site, *J. Mol. Biol. 334*, 477−488.
31. Garnett, A. P., and Viles, J. H. (2003) Copper Binding to the Octarepeats of the Prion Protein, *J. Biol. Chem. 278*, 6795−6802.

BI048555K